Am J Transl Res 2022;14(1):554-571
www.ajtr.org /ISSN:1943-8141/AJTR0136403

Original Article

Repair phase modeling of ischemic acute kidney injury: recovery vs. transition to chronic kidney disease

Kyungho Lee[1*], Hye Ryoun Jang[1*], Junseok Jeon[1], Kyeong Eun Yang[2], Jung Eun Lee[1], Ghee Young Kwon[3], Dae Joong Kim[1], Yoon-Goo Kim[1], Wooseong Huh[1]

[1]Division of Nephrology, Department of Medicine, Samsung Medical Center, Sungkyunkwan University School of Medicine, Seoul, Republic of Korea; [2]Division of Scientific Instrumentation & Management, Korea Basic Science Institute, Daejeon, Republic of Korea; [3]Department of Pathology, Samsung Medical Center, Sungkyunkwan University School of Medicine, Seoul, Republic of Korea. [*]Equal contributors and co-first authors.

Received June 15, 2021; Accepted December 7, 2021; Epub January 15, 2022; Published January 30, 2022

Abstract: The repair mechanism after ischemic acute kidney injury (AKI) involves complex immunologic processes, which determine long-term renal outcomes. Through investigating two murine ischemia-reperfusion injury (IRI) models: bilateral IRI (BIRI) and unilateral IRI (UIRI), we aimed to determine an appropriate murine model that could simulate the recovery phase of ischemic AKI. Changes in renal function, phenotypes of kidney mononuclear cells, renal fibrosis, and intrarenal cytokine/chemokine expression were serially analyzed up to 12 weeks after IRI. Plasma creatinine and BUN concentrations increased and remained elevated in the BIRI group until 7 days but decreased to comparable levels with the sham control group at 2 weeks after surgery and thereafter, whereas plasma creatinine and BUN concentrations remained unchanged in the UIRI group. Intrarenal total leukocytes, and effector memory and activated phenotypes of CD4 and CD8 T cells markedly increased in the postischemic kidneys in both IRI groups. Expression of proinflammatory cytokines/chemokines and TGF-β1 was enhanced in the postischemic kidneys of both IRI groups with a higher degree in the UIRI group. Importantly, intrarenal immunologic changes of the BIRI group persisted until 6 weeks despite full functional recovery. The postischemic kidneys of the UIRI group showed earlier and more pronounced proinflammatory conditions as well as more severe atrophic and fibrotic changes compared to the BIRI group. These findings support the utility of longer follow-ups of BIRI and UIRI models for investigating the adaptive repair process, which facilitates recovery of ischemic AKI and maladaptive repair process may result in AKI to CKD transition, respectively.

Keywords: Ischemic acute kidney injury, chronic kidney disease, ischemia-reperfusion injury, recovery, repair

Introduction

Ischemic acute kidney injury (AKI) is a major burden in both native kidneys and renal allografts due to its high mortality and lack of specific treatment [1]. While supportive measures such as dialysis and fluid therapy remain as the main management, treatments that will improve the clinical outcome are still in need [2]. Although AKI was previously recognized as a reversible condition, it is now a well-established risk factor for future CKD and end-stage renal disease (ESRD) [2, 3]. Incomplete or maladaptive repair of AKI causes AKI to CKD transition [4, 5]. Moreover, recent evidence highlighted that even reversible AKI with restored structural integrity and function can also increase the risk of CKD [6, 7]. Considering that the majority of AKI patients are diagnosed after an establishment of renal injury [8], therapeutic approaches targeting the repair phase may be clinically more important. Therefore, rigorous understanding of the repair mechanism is essential for developing clinically achievable therapeutic strategies.

Among various cellular and molecular mechanisms involved in AKI pathogenesis, intrarenal inflammatory responses are known to exert crucial roles determining renal outcome [9, 10]. Immune mechanisms involved in the repair process of ischemic AKI are believed to determine the fate of renal recovery [11, 12]. Moreover, as immune cells and their mediators are directly

linked to profibrotic pathways such as macrophage to myofibroblast transition [13], understanding their precise role during the repair phase is particularly important. To elucidate complex immune mechanisms of ischemic AKI [9, 10], various animal models have been utilized [14], of which murine ischemia-reperfusion injury (IRI) models have been most widely used [15-17]. Bilateral IRI (BIRI) model and unilateral IRI (UIRI) model have been commonly used to study early injury phase and long-term repair phase of ischemic AKI, respectively [18, 19]. Few studies have used the BIRI model to investigate the repair phase [20].

In this study, we hypothesized that a murine BIRI model may be more reliable than the UIRI model for studying adaptive repair processes, including the regeneration mechanism. Dynamic changes in intrarenal immunologic micromilieu in postischemic kidneys of the UIRI and BIRI models were compared. Depending on the time after ischemic insult, the goal is to determine the appropriate murine IRI model that could simulate the recovery phase of ischemic AKI.

Materials and methods

Animals

Male C57BL/6 mice were procured at the age of 9 weeks from Orient Bio Inc. (Seongnam, Kyoungki-do, Korea) and housed at the Animal Facility of Samsung Medical Center under specific pathogen-free conditions. This study protocol was approved by the Institutional Review Board of Samsung Medical Center (IACUC No. 20180222002) and the Samsung Medical Center Animal Care and Use Committee. Mice were randomly allocated to control, BIRI, and UIRI groups.

Renal IRI model

Established renal IRI models were used [15, 16]. Mice were anesthetized intraperitoneally using ketamine (100 mg/kg; Yuhan, Seoul, Korea) and xylazine (10 mg/kg; Bayer, Leverkusen, Germany). Renal pedicles were reached and isolated through an abdominal midline incision. In the BIRI model, both renal pedicles were clamped with microvascular clamps (Roboz Surgical Instrument, Gaithersburg, MD, USA) for 27 min. In the UIRI model, the left renal pedicle was clamped for 40 min. During the operation, mice were kept at a constant temperature (37°C) by a heating table and well hydrated with intraperitoneal injections of warm sterile saline. After clamping for the predetermined time, clamps were released and removed from the renal pedicles to allow reperfusion. After suturing, the mice were recovered with free access to chow and water. The surgical procedures were the same for the control animals, but renal pedicles were not clamped. Each cohort of mice was monitored and maintained for 1, 2, 4, 6, or 12 weeks before sacrifice.

Assessment of renal function

Blood samples were collected from tail veins on days 0, 1, 3, 7, 14, 21, 28, 42, 56, 70, and 84 days after surgery. Colorimetric kits were used to measure BUN (Fujifilm, Bedford, UK) and plasma creatinine (Arbor Assays, Ann Arbor, MI) concentrations according to the manufacturer's recommended methods.

Kidney histological analyses

After general anesthesia with ketamine (Yuhan) and xylazine (Bayer), exsanguination was performed, and the kidneys were harvested. Tissue sections were fixed with 10% phosphate buffered formalin, followed by staining with hematoxylin and eosin (H&E) and Masson's trichrome. Tubular damage and atrophy of the postischemic kidneys were assessed and scored by a renal pathologist under blinded conditions. The degree of interstitial fibrosis was scored semi-quantitatively for Masson's trichrome-stained slides using ImageJ 1.52k software (Wayne Rasband, National Institutes of Health, Bethesda, MD) and color deconvolution plug-in, as previously described [21, 22].

CD45 immunohistochemistry of renal tissues

Renal tissue sections were stained for CD45 immunohistochemistry as follows. After deparaffinizing and rehydrating tissue sections (4-μm-thick), they were transferred to citrate buffer solution (pH 6.0). The slides were then placed in a pressure cooker and heated with microwaves for 10 min. Subsequently, they were immersed in a hydrogen peroxide solution (DAKO, Carpinteria, CA) for 30 min and incubated overnight at 4°C with serum-free protein

block (DAKO). The slides were then incubated with a 1:100 anti-mouse CD45 monoclonal antibody (BD Biosciences) for 1 h at room temperature. The CD45-stained sections were incubated for 30 min at room temperature with a secondary antibody (REAL EnVision kit, DAKO) after rinsing. Subsequently, 3,3'-diaminobenzidine tetrahydrochloride (DAKO) was applied to the slides, and counterstained with Mayer's hematoxylin solution (DAKO). Whole fields of slides were scanned and analyzed to quantify the percentage of CD45-positive cells out of total nucleated cells by an automated computerized imaging analysis system, TissueFAXS (TissueGnostics, Vienna, Austria), as previously described [23].

Flow cytometry analysis of kidney-infiltrating mononuclear cells

KMNCs were isolated according to a previously established Percoll density gradient technique [24]. Briefly, decapsulated kidneys were suspended in RPMI buffer (Mediatech, Manassas, VA) containing 5% fetal bovine serum and mechanically disrupted using a Stomacher 80 Biosmaster (Sweward, Worthing, West Sussex, UK). Samples were strained through 70 μm cell strainers (BD Biosciences, San Jose, CA), washed, and resuspended in 36% Percoll (Amersham Pharmacia Biotech, Piscataway, NJ). Subsequently, the cells with 36% Percoll were gently laid over 72% Percoll. The samples were then centrifuged at 1,000×g for 30 min at room temperature. KMNCs were collected from the interface between 36% and 72% Percoll. The number of viable KMNCs was counted using an automated cell counter (Life Technologies, Bothell, WA).

Isolated KMNCs were resuspended in fluorescence-activated cell sorting (FACS) buffer and preincubated with anti-CD16/CD32 antibodies (BD Biosciences) for 10 min to avoid nonspecific antibody binding. KMNCs were then incubated with anti-mouse anti-CD3 (145-2C11), -CD4 (RM4-5), -CD8 (53-6.7), -CD19 (1D3), -CD25 (PC61), -CD44 (IM7), -CD45 (30-F11), -CD62L (MEL-14), -CD69 (H1.2F3), -Gr-1 (RB6-8C5), -F4/80 (T45-2342), -FoxP3 (MF-23), -TCRβ (H57-597), and -NK1.1 (PK136) (all from BD Biosciences) for 25 min at 4°C, and washed with FACS buffer. Sample data were acquired using a FACSVerse flow cytometer (BD Biosciences). Data were analyzed using FlowJo 10.7 software (BD Biosciences).

Multiplex cytokine/chemokine assay

Cytokines and chemokines were measured from kidney protein extracts by the multiplexed, particle-based, flow cytometric assay using Milliplex MAP Mouse Cytokine/Chemokine Kit (Luminex, Austin, TX) and Mouse Magnetic Luminex Assay Kit (R&D Systems, Minneapolis, MN) according to the manufacturer's instructions. IL-6, IL-10, monocyte chemoattractant protein (MCP)-1, regulated on activation, normal T cell expressed and secreted (RANTES, CCL5), TNF-α, and VEGF were analyzed. The intrarenal transforming growth factor (TGF)-β1 expression was measured using a mouse TGF-β1 DuoSet ELISA kit (R&D Systems) according to the manufacturer's instructions. The raw protein concentrations were measured using Pierce BCA protein assay kit (Thermo Fisher Scientific, Waltham, MA) to normalize each cytokine and chemokine concentrations.

Statistical analyses

Data are presented as the mean ± standard error of the mean (SEM). Differences between groups were analyzed using the one-way or two-way ANOVA followed by Tukey's post-hoc analysis or Mann-Whitney *U*-test. All statistical analyses were performed by GraphPad Prism 9 software (GraphPad Software, San Diego, CA). *P* values <0.05 were regarded statistically significant.

Results

Changes in renal function and kidney weight over time following renal IRI

Plasma creatinine and BUN concentrations increased sharply in the BIRI group, peaking on day 1, and remained higher than the control group for 7 days after IRI operation. On day 14 following the BIRI operation, plasma creatinine and BUN decreased to comparable levels to those in the control group (**Figure 1A**). Plasma creatinine and BUN concentrations in the UIRI group did not increase and were similar to those in the control group (**Figure 1B**).

As shown in **Figure 1C** and **1D**, there were significant atrophic changes in the left kidney and hypertrophy of the right kidney in the UIRI group. The weight of the left kidney was 25% of that of the right kidney.

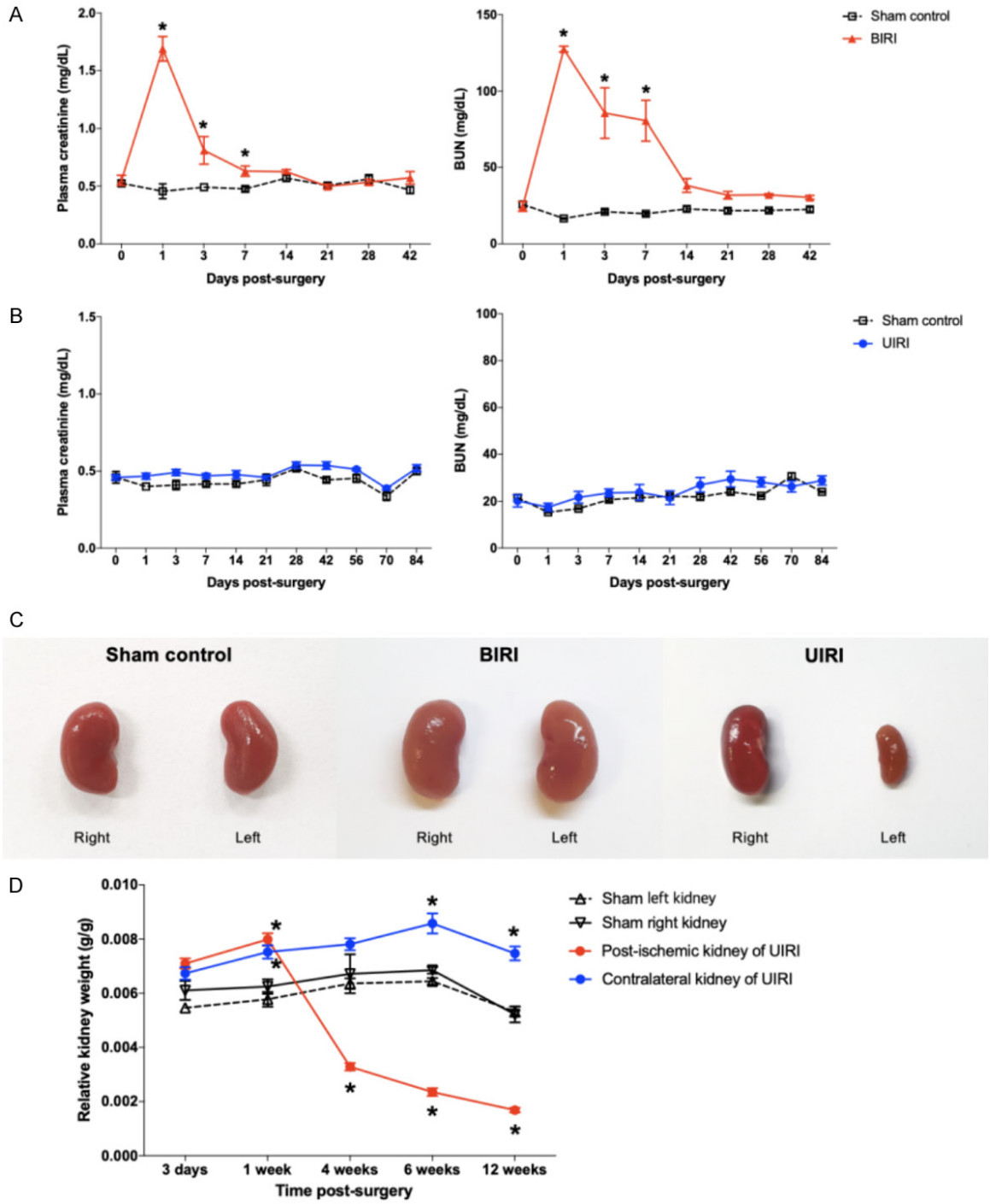

Figure 1. Serial follow-ups of renal function and kidney weights following IRI. A. Plasma creatinine and BUN concentrations of the BIRI group were elevated after IRI and significantly higher than those of the control group until 7 days. B. Plasma creatinine and BUN concentrations of the UIRI group were comparable with those of the control group during the whole follow-up period. $^{*}P<0.05$, compared with the control group (n=5-8 in each group). C. Representative gross kidney findings at 6 weeks after IRI. The postischemic kidney of the UIRI group (left kidney) showed significant atrophic change. D. The weights of the postischemic kidneys (left) in the UIRI group were significantly reduced during the recovery phase and lower than those of the control group and the contralateral kidneys from 4 weeks after IRI. Kidney weights were corrected for body weight. $^{*}P<0.05$, compared with the left kidney of the control group for the postischemic (left) kidney and the right kidney of the control for the contralateral (right) kidney of the UIRI group (n=4-8 in each group). Statistical analysis was performed using the Mann-Whitney U-test. BIRI, bilateral ischemia-reperfusion injury; BUN, blood urea nitrogen; IRI, ischemia-reperfusion injury; UIRI, unilateral ischemia-reperfusion injury.

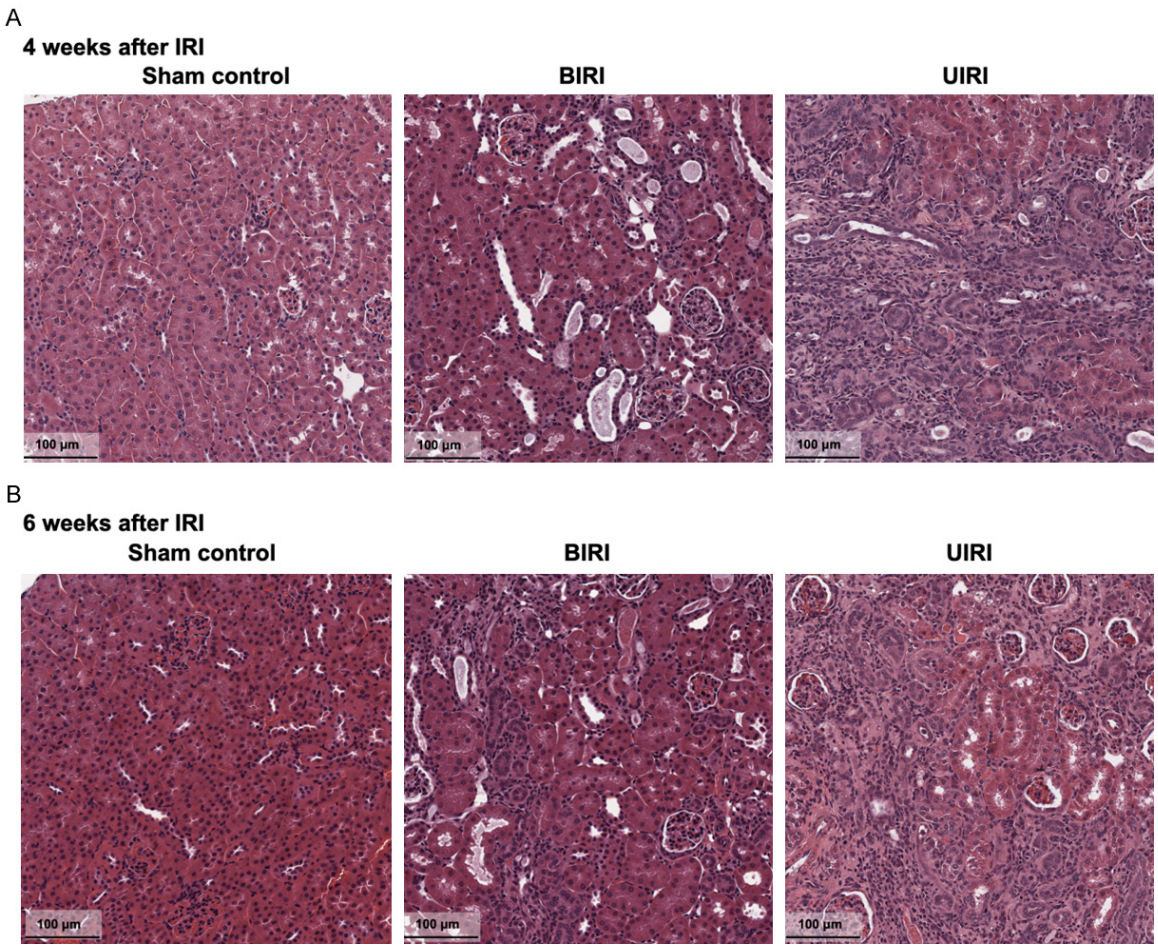

Figure 2. Structural renal injury following IRI. (A, B) Representative H&E staining findings of the postischemic kidneys at 4 weeks (A) and 6 weeks (B) after IRI. The postischemic kidneys of both IRI groups showed tubular damage, tubular atrophy, and inflammatory cell infiltration (×100).

Structural renal injury and fibrosis of two IRI models

H&E staining of postischemic kidneys in both IRI groups showed significant tubular damage, inflammatory cell infiltration, and tubular atrophy (**Figure 2A** and **2B**). There were more damaged tubules and atrophic tubules in the renal cortex and outer medulla in the UIRI group than in the BIRI group at 1 week, 4 weeks, and 6 weeks after IRI. The extent of damaged tubules and atrophic tubules did not progress after 2 weeks in the BIRI group and 4 weeks in the UIRI group (**Figure 3A** and **3B**).

Masson's trichrome stain revealed interstitial fibrosis in both IRI groups following IRI (**Figure 4A** and **4B**). The areas of the blue collagen fibers were quantified using a processed image of Masson's trichrome staining. Areas of fibrosis were significantly larger in the UIRI group than in the BIRI group at 1, 4, and 6 weeks after IRI. Areas of fibrosis in the UIRI group gradually increased until 6 weeks after IRI. Areas of fibrosis in the BIRI group did not progress from 1 week after IRI (**Figure 4C**).

Leukocyte trafficking into postischemic kidneys

Trafficked total leukocytes into postischemic kidneys were quantified by automated computerized analyzing system (TissueFAXS) with CD45 immunohistochemical stained slides (**Figure 5A** and **5B**). The percentage of total intrarenal leukocytes out of total nucleated cells increased significantly following IRI in both IRI groups compared to the control group. Kidney tissues from the UIRI group exhibited

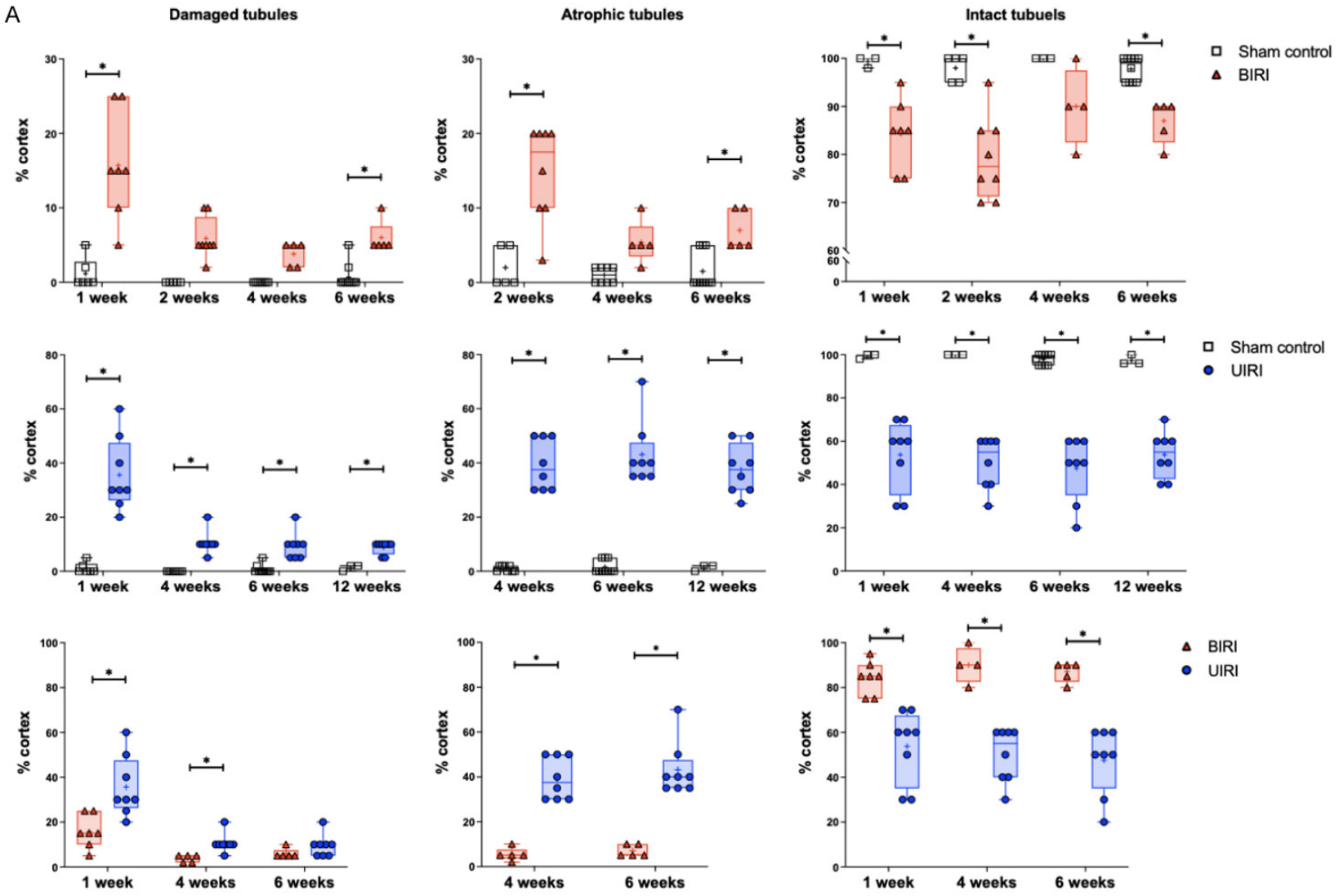
A
Damaged tubules
Atrophic tubules
Intact tubuels
% cortex
Sham control
BIRI
UIRI
1 week
2 weeks
4 weeks
6 weeks
12 weeks

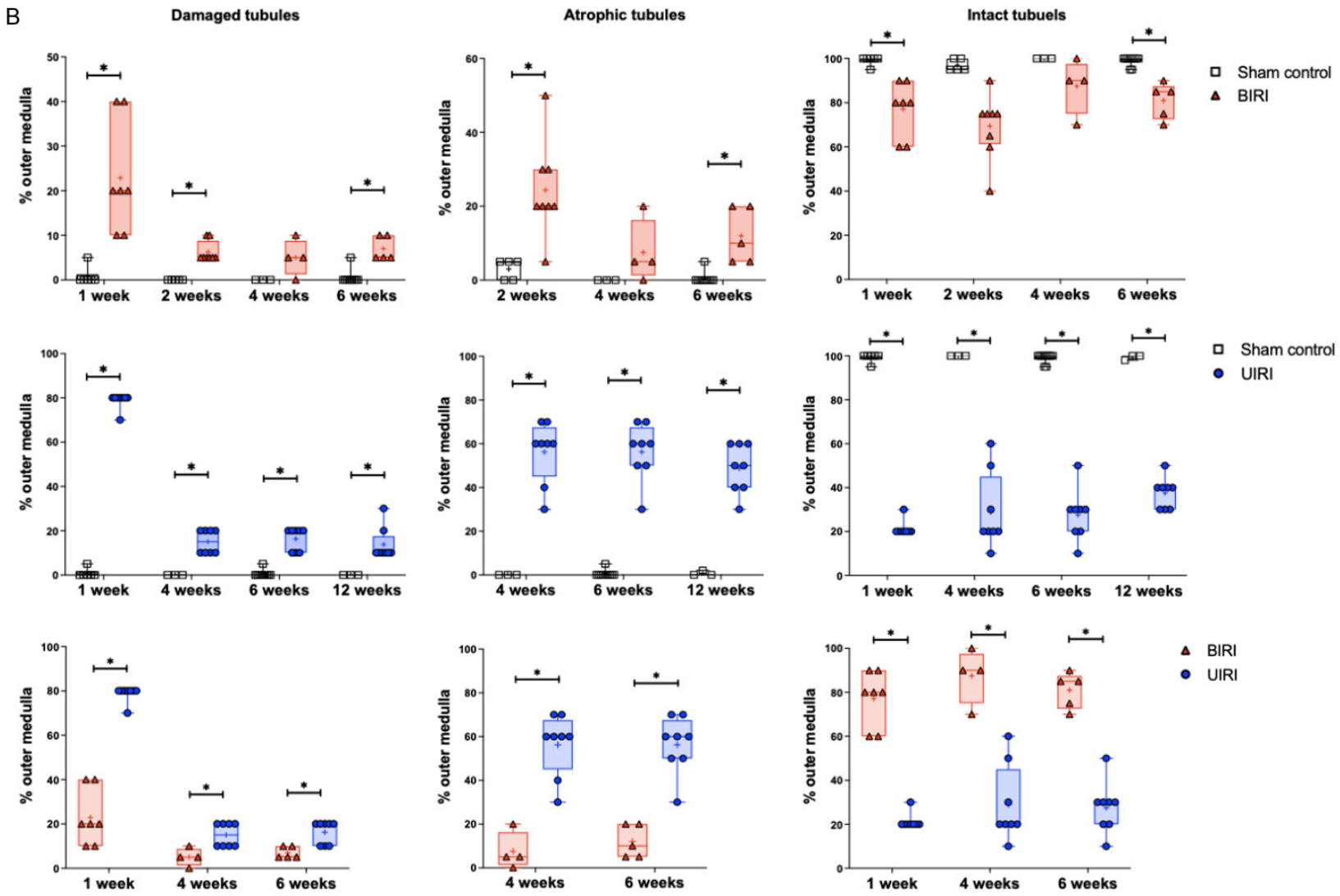

Figure 3. Quantitative analyses of structural renal injury in renal cortex and outer medulla. (A, B) Comparison of proportions of damaged tubules, atrophic tubules, and intact tubules for each group in renal cortex (A) and outer medulla (B). Tubular damage and atrophic changes were significant in both IRI groups. The proportions of damaged tubules and atrophic tubules in the renal cortex and outer medulla were significantly higher in the UIRI group than those of the BIRI group at each time point. A total of 10 magnified fields (×200) were scored for each mouse by a pathologist blinded to the groups. Data are from four independent experiments. The boxplots display the IQR and median (+, mean). Whiskers describe minimum to maximum range. $^{*}P<0.05$ (n=5-8 in each group). Statistical analysis was performed using the Mann-Whitney U test. BIRI, bilateral ischemia-reperfusion injury; IRI, ischemia-reperfusion injury; UIRI, unilateral ischemia-reperfusion injury; IQR, interquartile range.

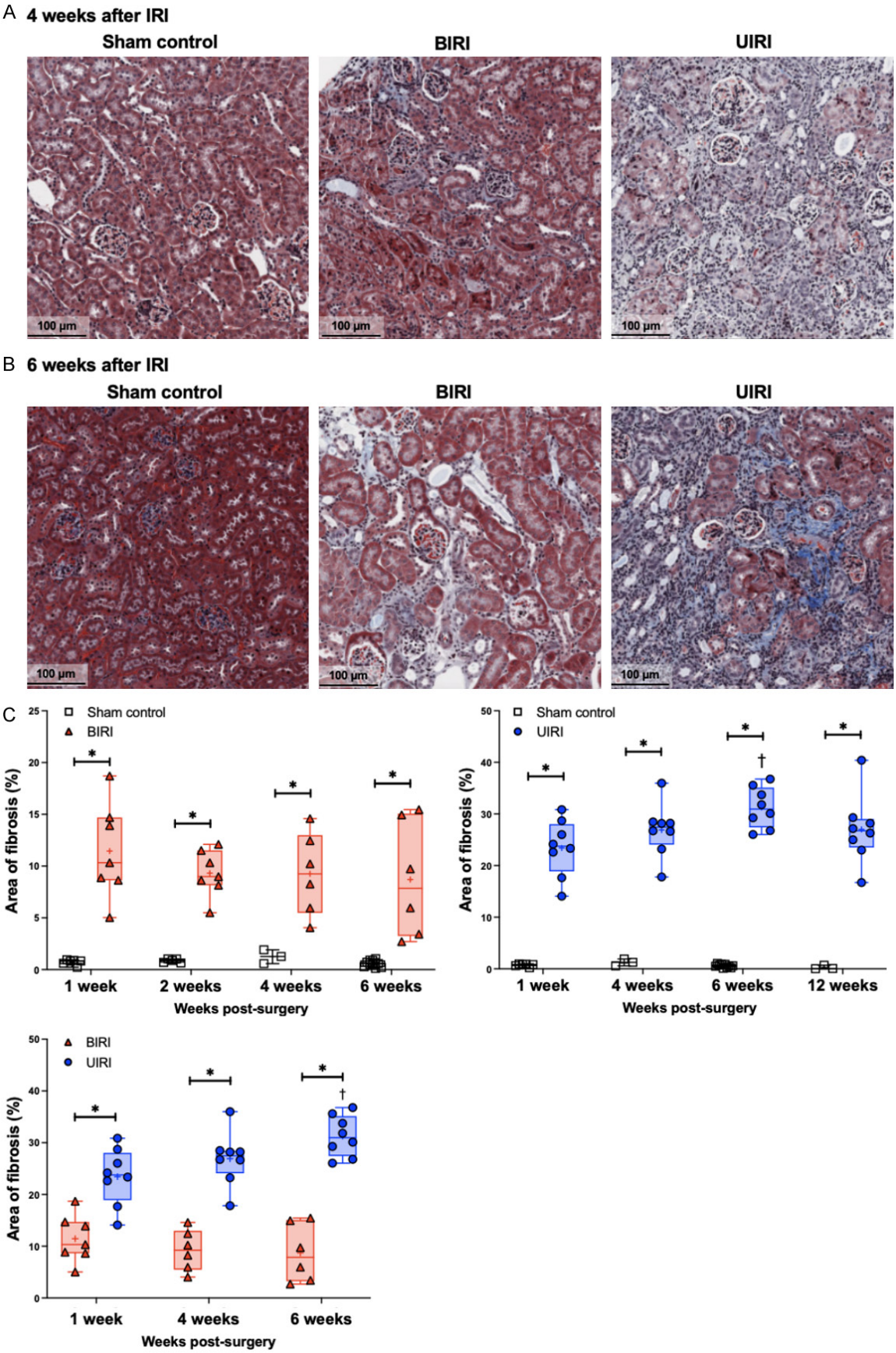
A 4 weeks after IRI
Sham control
BIRI
UIRI
100 μm
B 6 weeks after IRI
Sham control
BIRI
UIRI
100 μm
C
Sham control
BIRI
Area of fibrosis (%)
1 week
2 weeks
4 weeks
6 weeks
Weeks post-surgery
Sham control
UIRI
Area of fibrosis (%)
1 week
4 weeks
6 weeks
12 weeks
Weeks post-surgery
BIRI
UIRI
Area of fibrosis (%)
1 week
4 weeks
6 weeks
Weeks post-surgery

Figure 4. Renal fibrosis following IRI. A, B. Representative images of Masson's trichrome staining at 4 and 6 weeks after IRI. The postischemic kidneys of both IRI models showed interstitial fibrosis (Masson's trichrome-stained slides showing fibrosis with blue color, ×100). C. Calculated areas of fibrosis for each group. The area of blue collagen fibers was quantified using software analyses of processed images of Masson's trichrome staining. Both IRI groups showed significant fibrotic changes compared to the control group at each time point. Fibrotic area for the UIRI group showed an increasing trend until 6 weeks after IRI and was significantly greater than for the BIRI group at 1, 4, and 6 weeks. The boxplots display the IQR and median (+, mean). Whiskers describe minimum to maximum range. $^{*}P<0.05$, between two groups at each time point; $^{\dagger}P<0.05$, compared with 1 week in the same group (n=5-7 in each group). Statistical analysis was performed using the Mann-Whitney U-test. BIRI, bilateral ischemia-reperfusion injury; IRI, ischemia-reperfusion injury; UIRI, unilateral ischemia-reperfusion injury; IQR, interquartile range.

the most prominent leukocyte infiltration compared to the BIRI group at both 4 and 6 weeks after IRI (**Figure 5C**).

Differences in the intrarenal leukocyte phenotypes depending on IRI models

The proportions of innate and adaptive immune cells in the postischemic kidneys were analyzed at 1, 4, 6, and 12 weeks after IRI. The proportion of total T cells among total lymphocytes in the postischemic kidneys increased during the recovery phase and was higher in the UIRI group than in the BIRI group. The proportion of total B cells among total lymphocytes of the UIRI group gradually decreased after IRI and remained lower compared to both the control and BIRI groups. Intrarenal neutrophil infiltration was higher in the UIRI group than in the control and BIRI groups, and reached a peak at 6 weeks after IRI. Neutrophil infiltration in the BIRI group was comparable to that in the control group (**Figure 6A** and **6B**).

The proportion of CD4 T cells among the total T cells increased in the postischemic kidneys of both IRI groups. Effector memory and activated CD4 and CD8 T cells markedly increased among total CD4 and CD8 T cells in the postischemic kidney of both IRI groups. These changes started earlier and were more prominent in the UIRI group. The proportion of regulatory T cells among CD4 T cells in both IRI groups also increased during the recovery phase (**Figure 7A** and **7B**).

Intrarenal expressions of cytokines/chemokines depending on IRI models

Intrarenal expression of proinflammatory cytokines/chemokines, including MCP-1, RANTES, TNF-α, and IL-6, was more significant in the UIRI group than in the control and BIRI groups. In contrast, the expression of VEGF was significantly lower in the UIRI group than in the control and BIRI groups (**Figure 8A**).

The expression of intrarenal TGF-β1 also increased in both IRI groups. In the UIRI group, TGF-β1 was significantly higher than in the BIRI group at 1 and 4 weeks after IRI, and remained elevated until 12 weeks (**Figure 8B**).

Discussion

In this study, the BIRI and UIRI models were thoroughly analyzed so as to determine a more appropriate murine model for investigating the repair processes of ischemic AKI. Postischemic kidneys from both renal IRI models generated long-term immunological and histological changes with increased trafficking of total leukocytes. The immunologic changes included facilitated infiltration of effector memory and activated phenotypes of T cells and regulatory T cells. The UIRI group showed significantly profibrotic and atrophic responses, indicating a maladaptive repair process would result in AKI-CKD transition. The BIRI group showed less fibrosis and atrophic changes with lower expression of proinflammatory cytokines/chemokines, including TGF-β1, compared with the UIRI group. Although the BIRI group exhibited functionally reversible AKI within 2 weeks, the intrarenal proinflammatory micromilieu persisted until 6 weeks after IRI. These results suggest that BIRI model is more likely to be suitable for investigating adaptive repair and regeneration processes during the recovery phase, whereas the UIRI model may represent maladaptive repair and fibrosis better than the BIRI model.

During the recovery phase, intrarenal lymphocytes underwent dynamic changes in their subtypes and functional characteristics. Trafficking of T cells, especially activated and effector memory phenotypes of CD4 and CD8 T cells, increased in the postischemic kidneys from

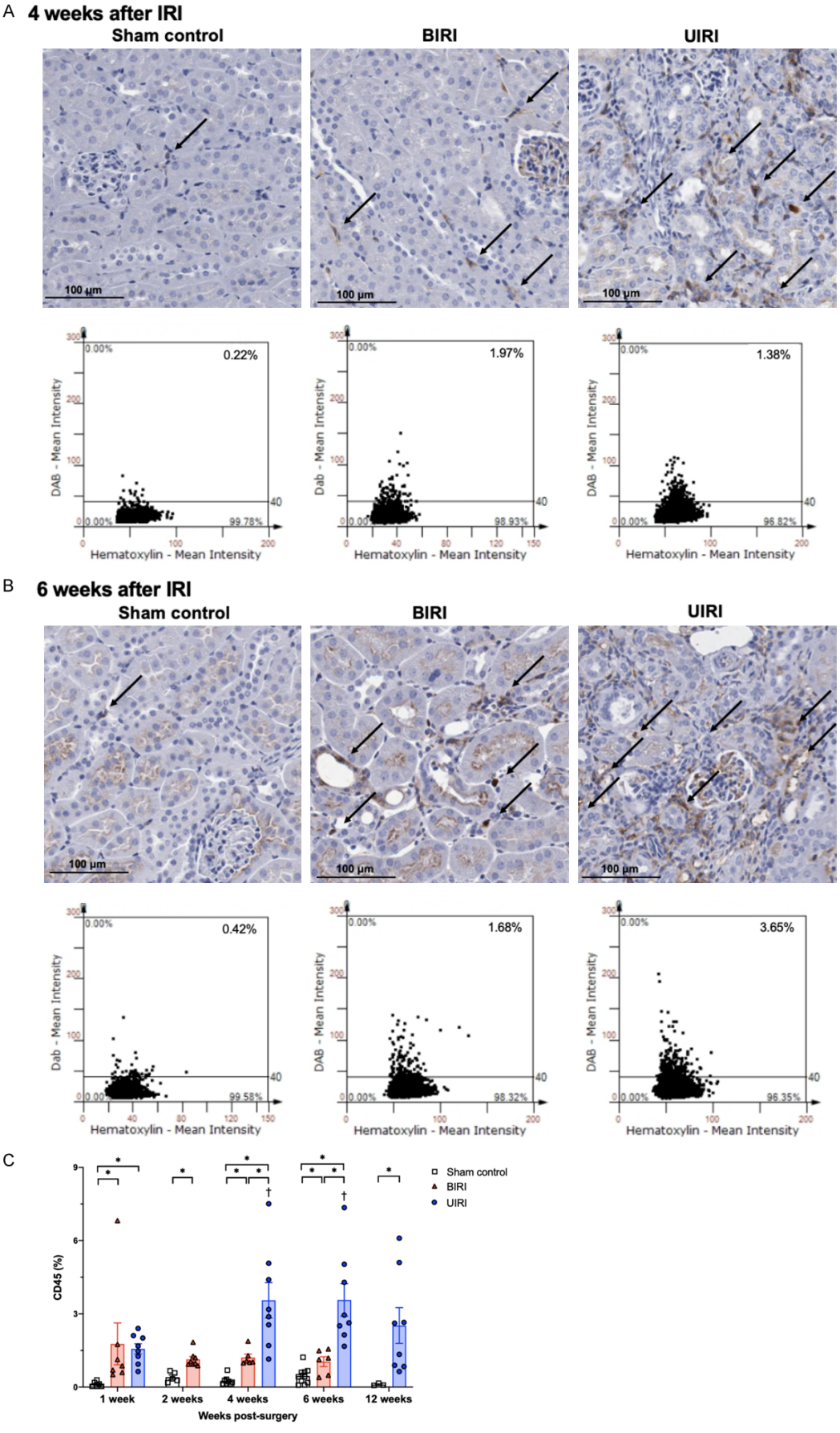
A
4 weeks after IRI
Sham control
BIRI
UIRI
100 μm
0.22%
1.97%
1.38%
DAB - Mean Intensity
Hematoxylin - Mean Intensity
B
6 weeks after IRI
Sham control
BIRI
UIRI
100 μm
0.42%
1.68%
3.65%
C
CD45 (%)
Weeks post-surgery
1 week
2 weeks
4 weeks
6 weeks
12 weeks
Sham control
BIRI
UIRI

Figure 5. Intrarenal leukocytes trafficked into the postischemic kidneys. A, B. Representative immunohistochemistry findings and semiquantitative analyses of CD45-positive leukocytes with tissue FAXS in the postischemic kidneys at 4 and 6 weeks after IRI. Arrows indicate CD45-positive leukocytes (×200). C. Semiquantitative analysis of CD45-positive leukocytes using an automated imaging analysis system (TissueFAXS). The whole fields of slides including both the cortex and medulla were calculated. The proportions of total leukocytes expressing CD45 among total nucleated cells were higher in both IRI groups than in the control group at each time point. The UIRI group showed a greater increase compared to the BIRI group at 4 and 6 weeks after IRI. Data are from four independent experiments. $^{*}P<0.05$, between the groups at each time point; $^{\dagger}P<0.05$, compared with 1 week in the same group (n=6-10 in each group). Statistical analysis was performed using the Mann-Whitney U-test. BIRI, bilateral ischemia-reperfusion injury; CD, cluster of differentiation; IRI, ischemia-reperfusion injury; UIRI, unilateral ischemia-reperfusion injury.

both IRI groups. The UIRI group showed earlier and more prominent infiltration of T cells compared to the BIRI group. These phenotypic switches of T cells have been considered to be involved in prolonged responses to damage-associated molecular pattern-associated self-antigens and repair process [10, 25]. Infiltration of regulatory T cells, which are known to have proregenerative function in IRI [10-12], increased in the recovery phase in both IRI models. The peak proportion of regulatory T cells was higher in the BIRI group at 6 weeks than in the UIRI group. Intriguingly, these phenotypic changes in T cells were sustained at 6 weeks after IRI despite complete recovery of renal function in the BIRI model. This finding may indicate that the repair and regeneration processes are still ongoing, even after full functional recovery from ischemic AKI.

Neutrophils, major effector cells of innate immunity, are known to contribute to tissue damage [26] and participate in the pathogenesis of renal IRI [27]. Prominent long-term infiltration of neutrophils was found only in the UIRI model and may contribute to a maladaptive repair process by extending the inflammatory response. Moreover, the UIRI group showed enhanced expression of proinflammatory cytokines/chemokines and reduced expression of a protective cytokine VEGF [28, 29]. These findings correlated with the histologic features of the UIRI group, showing profound inflammatory cell infiltration and fibrosis.

The UIRI model has been widely used to investigate the recovery phase with longer follow-up duration because uninjured contralateral kidney allows to achieve long-term survival [19, 30-32]. However, the UIRI model showed two critical limitations. First, there was no increase in plasma creatinine or BUN concentrations despite the profound renal fibrosis in the postischemic kidney. Second, the observed significant weight reduction of the postischemic kidney in the UIRI model reflected this maladaptive repair, which makes it difficult to study the active regeneration process. It has been recently reported that redistribution of renal blood flow due to existence of intact contralateral kidney contributes maladaptive repair process of unilateral IRI [33]. The functional compensation of uninjured contralateral kidney is more likely to inhibit active regeneration of injured kidney. As renal fibrosis and atrophic changes are hallmarks of CKD [34], the UIRI model seems to be more appropriate for investigating the mechanisms of AKI to CKD transition [19, 30] rather than adaptive repair and regeneration. Notably, atrophic tubules and the degree of fibrosis in the UIRI model did not progress after 6 weeks from IRI, which may suggest that a maximum of 6-week follow-up duration would be acceptable for immunologic studies targeting the recovery phase using this model.

Although it has been reported that the contralateral kidney can undergo cellular changes that serves as compensatory function [30], the phenotypes of KMNCs in the contralateral kidney of the UIRI group were similar to those from the control mice in our study.

The BIRI model showed less severe fibrosis and atrophic changes than the UIRI model. The postischemic kidneys of the BIRI group seemed to be more capable of complete restoration of function after IRI than the UIRI model. Functional assessment was available to compare the severity of AKI in each of the mice. Since the development of the uremic milieu is the most crucial pathophysiologic feature of human AKI [18], the BIRI model may be more representative of clinical AKI. Furthermore, the uremic milieu *per se* can affect the immune

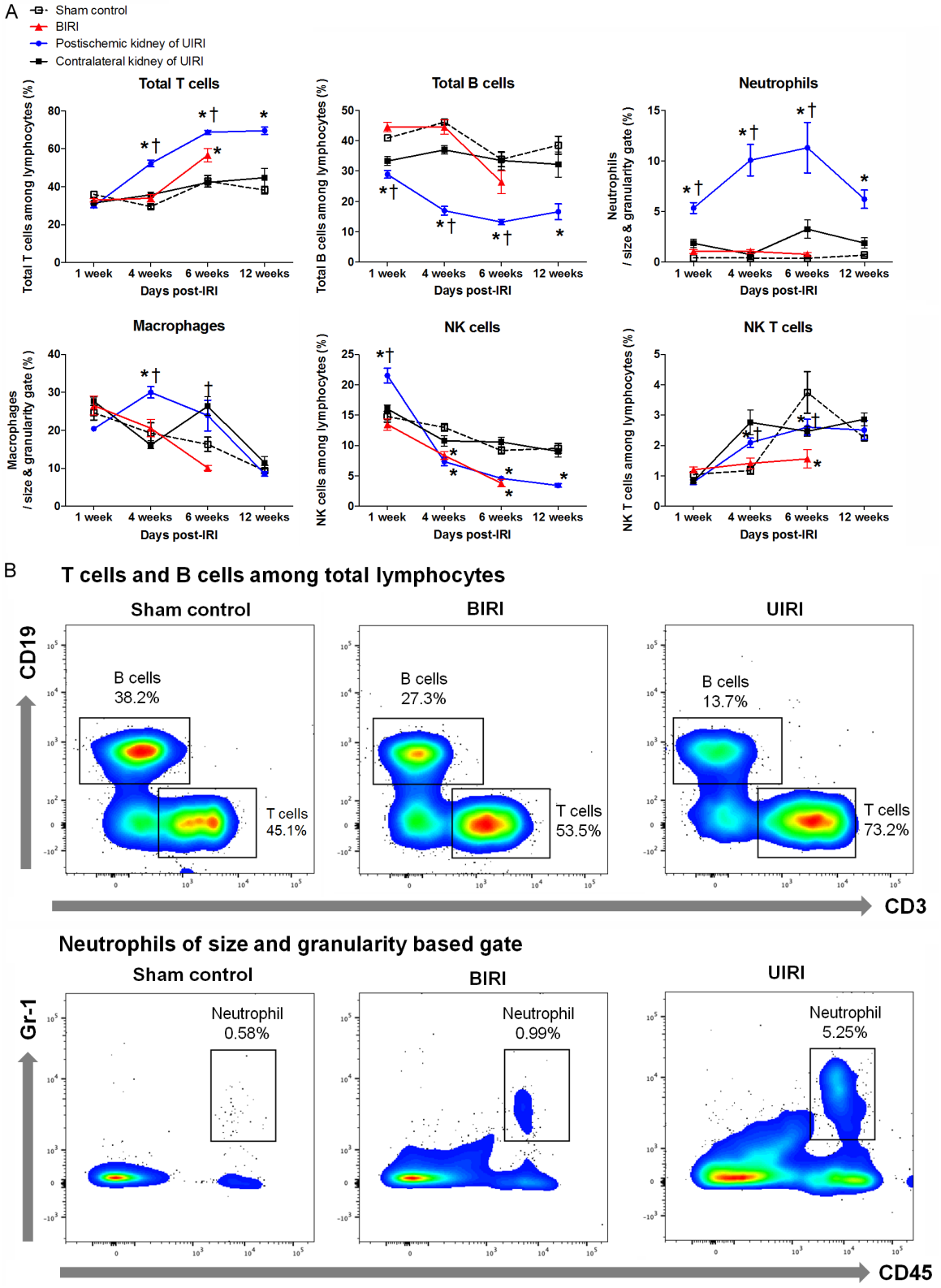

Figure 6. Flow cytometry analyses of KMNCs isolated from postischemic kidneys. A. Changes in subpopulations of KMNCs according to the IRI models. The proportion of total T cells among total lymphocytes increased in both IRI groups. The UIRI group showed relatively reduced infiltration of total B cells and facilitated infiltration of neutrophils. B. Representative flow plots showing T cells, B cells, and neutrophils at 6 weeks after IRI. $^{*}P<0.05$, compared with the control group; $^{\dagger}P<0.05$, compared with the BIRI group (n=7-8 in each group). Statistical analyses were performed using ANOVA followed by Tukey's post-hoc analysis. BIRI, bilateral ischemia-reperfusion injury; KMNCs, kidney-infiltrating mononuclear cells; IRI, ischemia-reperfusion injury; UIRI, unilateral ischemia-reperfusion injury.

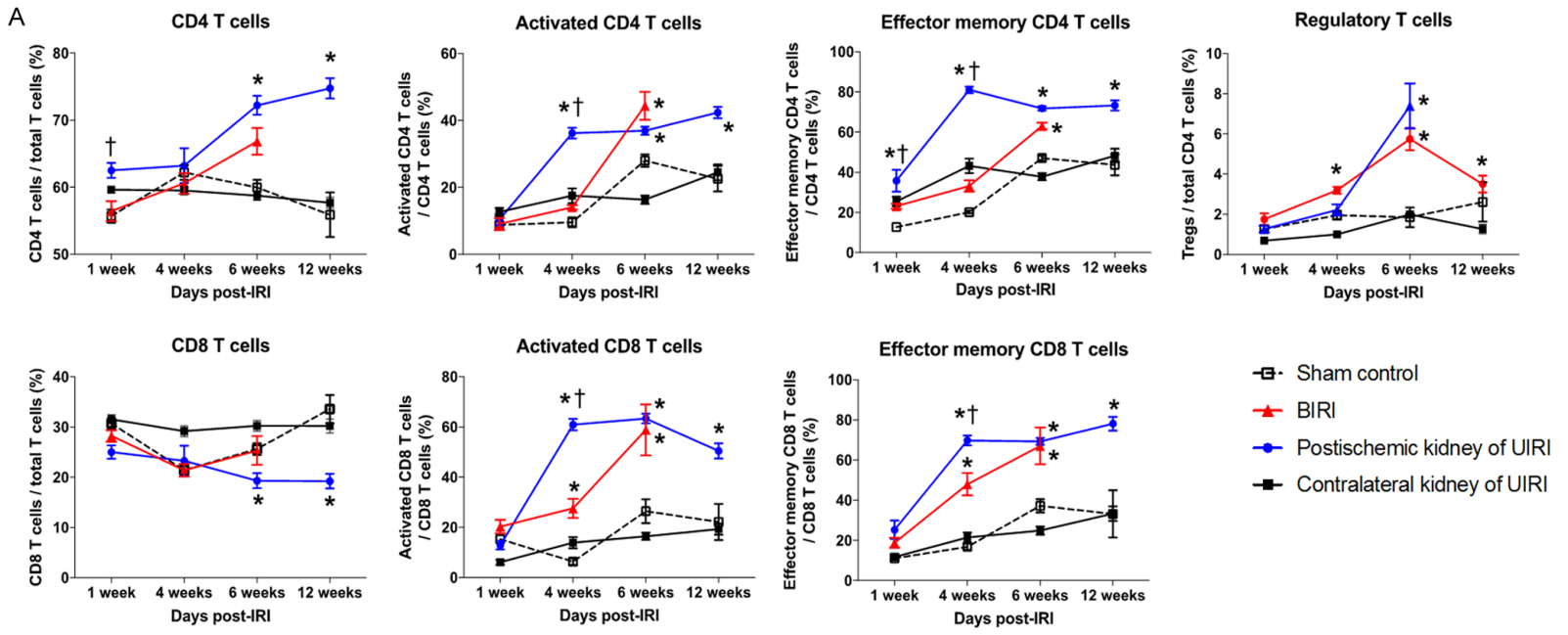
A
CD4 T cells
CD4 T cells / total T cells (%)
Activated CD4 T cells
Activated CD4 T cells / CD4 T cells (%)
Effector memory CD4 T cells
Effector memory CD4 T cells / CD4 T cells (%)
Regulatory T cells
Tregs / total CD4 T cells (%)
CD8 T cells
CD8 T cells / total T cells (%)
Activated CD8 T cells
Activated CD8 T cells / CD8 T cells (%)
Effector memory CD8 T cells
Effector memory CD8 T cells / CD8 T cells (%)
1 week
4 weeks
6 weeks
12 weeks
Days post-IRI
Sham control
BIRI
Postischemic kidney of UIRI
Contralateral kidney of UIRI

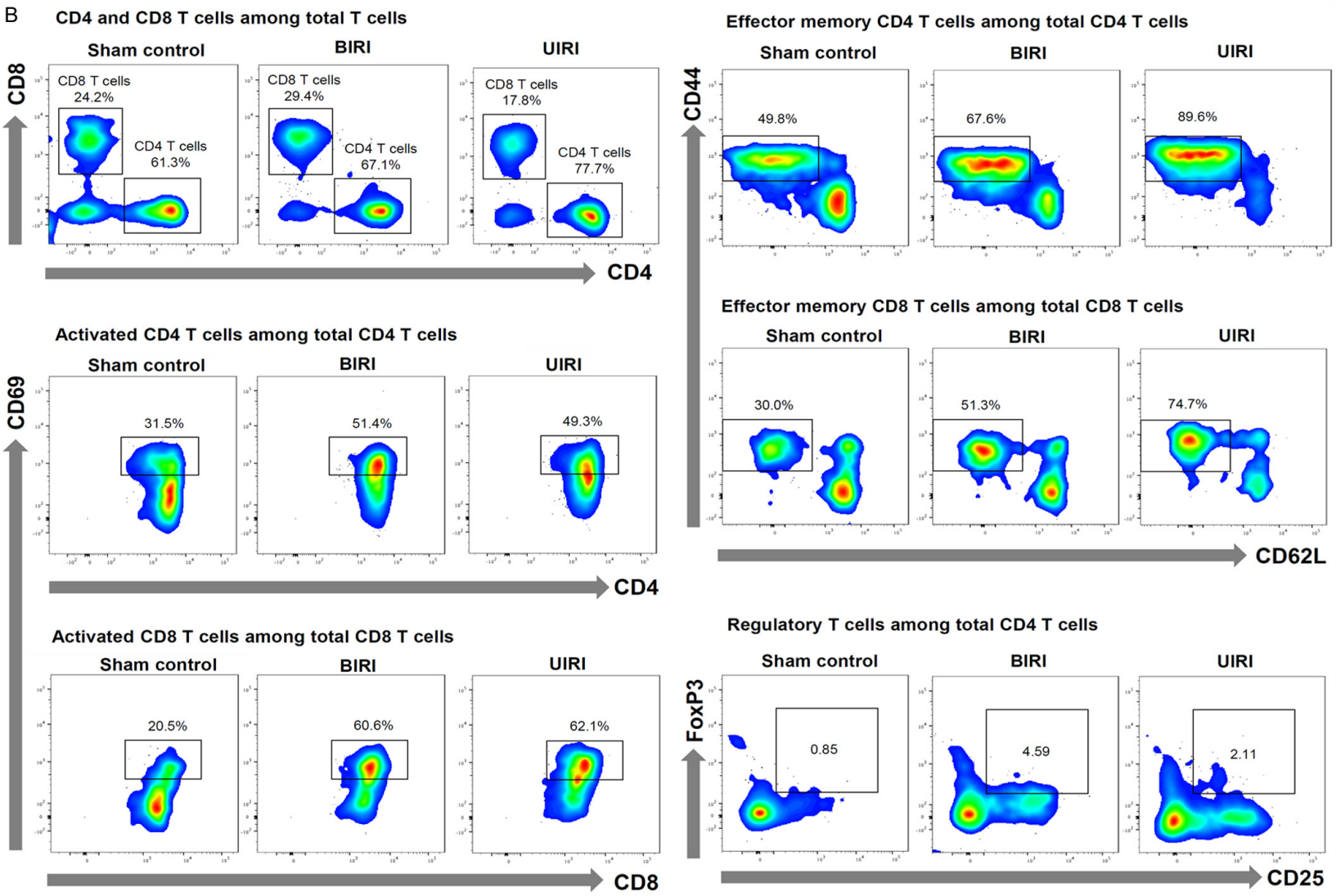

Figure 7. Flow cytometry analyses of postischemic kidney T cell subpopulations. A. Changes in intrarenal T cell subpopulations according to the IRI models. Effector memory CD4 and CD8 T cells, activated CD4 and CD8 T cells, and regulatory T cells markedly increased in the postischemic kidneys in both IRI groups. B. Representative flow plots showing CD4 and CD8 T cells, activated and effector memory subsets of CD4 and CD8 T cells, and regulatory T cells at 6 weeks after IRI. $^{*}P<0.05$, compared with the control group; $^{\dagger}P<0.05$, compared with the BIRI group (n=7-8 in each group). Statistical analyses were performed using ANOVA followed by Tukey's post-hoc analysis. BIRI, bilateral ischemia-reperfusion injury; KMNCs, kidney-infiltrating mononuclear cells; IRI, ischemia-reperfusion injury; UIRI, unilateral ischemia-reperfusion injury.

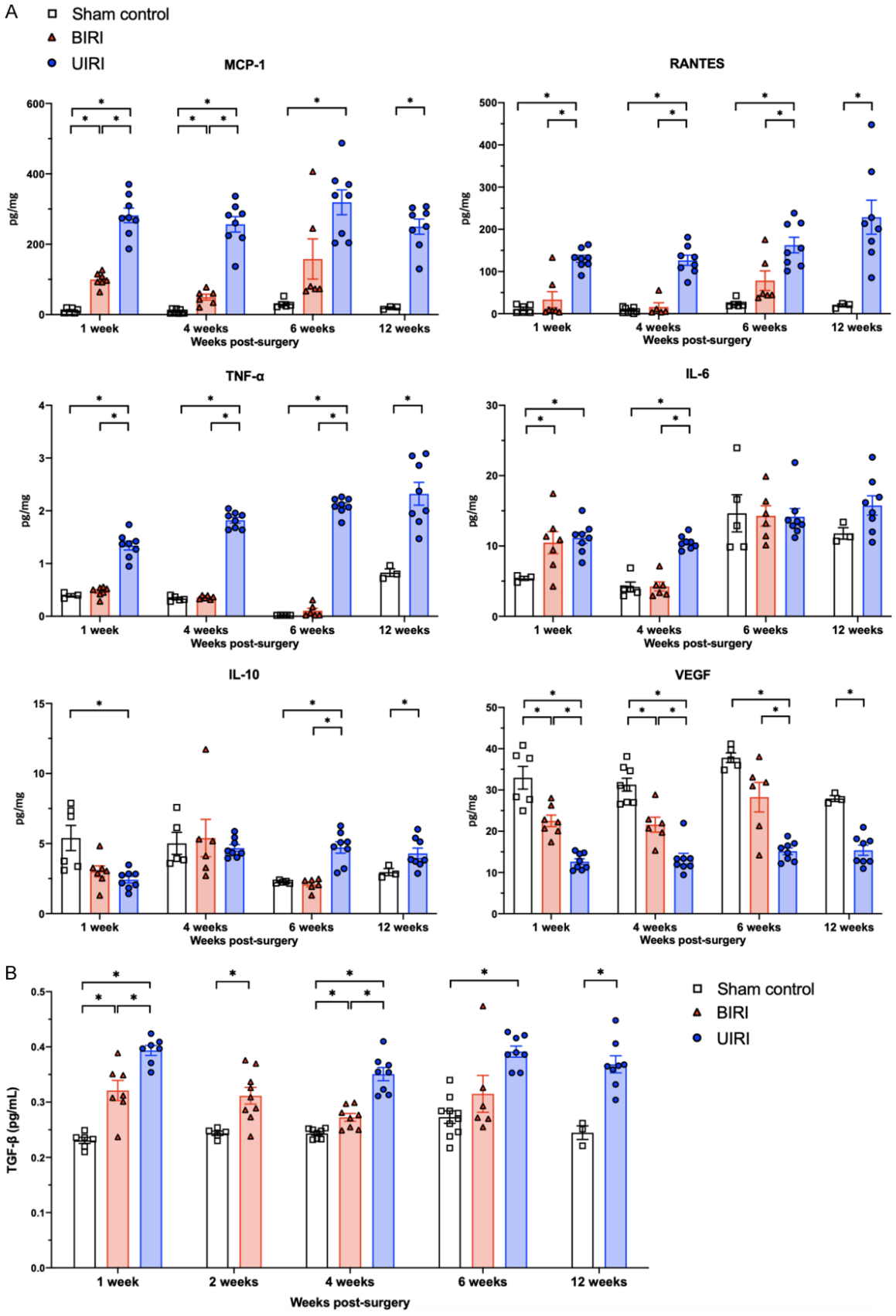
A
Sham control
BIRI
UIRI
MCP-1
RANTES
TNF-α
IL-6
IL-10
VEGF
pg/mg
1 week
4 weeks
6 weeks
12 weeks
Weeks post-surgery
B
TGF-β (pg/mL)
2 weeks

Figure 8. Expressions of intrarenal cytokines/chemokines and TGF-β1 following IRI. A. The expression of MCP-1, RANTES, TNF-α, and IL-6 were significantly higher in the UIRI group than those in the control and BIRI groups. The expression of VEGF was lower in the UIRI group than that in the control and BIRI groups. $^{*}P<0.05$ (n=5-8 in each group). Statistical analyses were performed using ANOVA followed by Tukey's post-hoc analysis. B. The expression of TGF-β1 was significantly higher in the UIRI group than in the control and BIRI groups (n=5-10 in each group). Statistical analyses were performed using ANOVA followed by Tukey's post-hoc analysis. BIRI, bilateral ischemia-reperfusion injury; IRI, ischemia-reperfusion injury; MCP-1, monocyte chemoattractant protein-1; RANTES, regulated on activation, normal T cell expressed and secreted (CCL5); UIRI, unilateral ischemia-reperfusion injury; TGF-β1, transforming growth factor-β1.

response following IRI by which alters the renal recovery process [35, 36]. AKI induced distant organ dysfunction also highlighted the significance of the AKI-induced uremic milieu in mechanistic studies of AKI [37]. Taken together with the comparative results with the UIRI model, the BIRI model with longer follow-up of 2-6 weeks may be more suitable for studying the active repair and regeneration process following IRI.

Our study has a few limitations. First, although we focused on the dynamic changes in intrarenal infiltration of immune cells, the precise roles of the immune cells that increased during the repair phase were not fully elucidated. Further studies are warranted to evaluate the precise mechanism of each immune cell during the recovery process following renal IRI. Second, other modified models such as UIRI with contralateral nephrectomy [38-40] and two-stage BIRI [41] were not evaluated. However, such models require complicated and cumbersome procedures [40, 41] and are associated with high surgical mortality, making it difficult to achieve long-term survival to study the recovery phase [32, 40]. Third, a single relevant ischemic time and temperature were used for each IRI model during the operation. Since ischemic time and temperature affect renal outcome after IRI, modifications to them may result in different results [19]. Further studies using different ischemic times and temperatures would be helpful to simulate more ideal models according to the main purposes of the IRI study.

Dynamic changes in histologic findings and intrarenal immune responses following IRI were demonstrated in the two distinct IRI models. The UIRI model showed profound atrophy and fibrosis, reflecting a maladaptive repair process and a direct AKI-CKD transition. The BIRI model generated dynamic and chronic changes in intrarenal immunologic micromilieu despite complete restoration of renal function and mild structural injury, simulating reversible episodes of human AKI. Our comprehensive study suggests that the BIRI model may be more appropriate for investigating the adaptive repair process of ischemic AKI, and the UIRI model may be preferable for investigating the transition of AKI to CKD.

Acknowledgements

We deeply appreciate the great technical support of Kyungyi Choi, Ji Woo Kim, and Wu Hyun Lee at the Samsung Biomedical Research Institute, Samsung Medical Center, Sungkyunkwan University School of Medicine. Kyungho Lee was supported by a grant from the Korea Health Technology R&D Project through the Korea Health Industry Development Institute, funded by the Ministry of Health & Welfare, Republic of Korea (grant number: HI19C1337). Hye Ryoun Jang was supported by the National Research Foundation of the Republic of Korea (grant number: 2016R1A2B4008235 & 2019-R1A2B5B01069346). Wooseoung Huh was supported by the National Research Foundation of the Republic of Korea (grant number: 2017R1D1A1B04032172). This study was supported by the National Research Foundation of Korea (grant numbers NRF-2016R1A-2B4008235, 2019R1A2B5B01069346, and 2017R1D1A1B04032172).

Disclosure of conflict of interest

None.

Abbreviations

AKI, acute kidney injury; BIRI, bilateral ischemia-reperfusion injury; BUN, blood urea nitrogen; CKD, chronic kidney disease; H&E, hematoxylin and eosin; HK-2 cell, human kidney-2 cell; IQR, interquartile range; IRI, ischemia-reperfusion injury; KMNCs, kidney mononucle-

ar cells; MCP-1, monocyte chemoattractant protein-1; RANTES, regulated on activation, normal T cell expressed and secreted; SEM, standard error of the mean; TGF-β, transforming growth factor-β; TLR, toll-like receptor; UIRI, unilateral ischemia-reperfusion injury.

Address correspondence to: Dr. Wooseong Huh, Division of Nephrology, Department of Medicine, Samsung Medical Center, Sungkyunkwan University School of Medicine, 81, Irwon-Ro, Gangnam-Gu, Seoul, Republic of Korea. Tel: +82-234103443; Fax: +82-234100064; E-mail: wooseong.huh@samsung.com

References

[1] Palevsky PM, Zhang JH, O'Connor TZ, Chertow GM, Crowley ST, Choudhury D, Finkel K, Kellum JA, Paganini E, Schein RM, Smith MW, Swanson KM, Thompson BT, Vijayan A, Watnick S, Star RA and Peduzzi P. Intensity of renal support in critically ill patients with acute kidney injury. N Engl J Med 2008; 359: 7-20.

[2] Kurzhagen JT, Dellepiane S, Cantaluppi V and Rabb H. AKI: an increasingly recognized risk factor for CKD development and progression. J Nephrol 2020; 33: 1171-1187.

[3] Ishani A, Xue JL, Himmelfarb J, Eggers PW, Kimmel PL, Molitoris BA and Collins AJ. Acute kidney injury increases risk of ESRD among elderly. J Am Soc Nephrol 2009; 20: 223-228.

[4] Yang L, Besschetnova TY, Brooks CR, Shah JV and Bonventre JV. Epithelial cell cycle arrest in G2/M mediates kidney fibrosis after injury. Nat Med 2010; 16: 535-543.

[5] Kumar S. Cellular and molecular pathways of renal repair after acute kidney injury. Kidney Int 2018; 93: 27-40.

[6] Bucaloiu ID, Kirchner HL, Norfolk ER, Hartle JE 2nd and Perkins RM. Increased risk of death and de novo chronic kidney disease following reversible acute kidney injury. Kidney Int 2012; 81: 477-485.

[7] Kellum JA. Persistent acute kidney injury. Crit Care Med 2015; 43: 1785-1786.

[8] Thomas ME, Blaine C, Dawnay A, Devonald MA, Ftouh S, Laing C, Latchem S, Lewington A, Milford DV and Ostermann M. The definition of acute kidney injury and its use in practice. Kidney Int 2015; 87: 62-73.

[9] Jang HR, Ko GJ, Wasowska BA and Rabb H. The interaction between ischemia-reperfusion and immune responses in the kidney. J Mol Med (Berl) 2009; 87: 859-864.

[10] Jang HR and Rabb H. Immune cells in experimental acute kidney injury. Nat Rev Nephrol 2015; 11: 88-101.

[11] Gharaie Fathabad S, Kurzhagen JT, Sadasivam M, Noel S, Bush E, Hamad ARA and Rabb H. T lymphocytes in acute kidney injury and repair. Semin Nephrol 2020; 40: 114-125.

[12] Lee SA, Noel S, Sadasivam M, Hamad ARA and Rabb H. Role of immune cells in acute kidney injury and repair. Nephron 2017; 137: 282-286.

[13] Tang PM, Nikolic-Paterson DJ and Lan HY. Macrophages: versatile players in renal inflammation and fibrosis. Nat Rev Nephrol 2019; 15: 144-158.

[14] Lieberthal W and Nigam SK. Acute renal failure. II. Experimental models of acute renal failure: imperfect but indispensable. Am J Physiol Renal Physiol 2000; 278: F1-F12.

[15] Jang HR, Gandolfo MT, Ko GJ, Satpute SR, Racusen L and Rabb H. B cells limit repair after ischemic acute kidney injury. J Am Soc Nephrol 2010; 21: 654-665.

[16] Jang HR, Park JH, Kwon GY, Park JB, Lee JE, Kim DJ, Kim YG, Kim SJ, Oh HY and Huh W. Aging has small effects on initial ischemic acute kidney injury development despite changing intrarenal immunologic micromilieu in mice. Am J Physiol Renal Physiol 2016; 310: F272-283.

[17] Kinsey GR, Sharma R and Okusa MD. Regulatory T cells in AKI. J Am Soc Nephrol 2013; 24: 1720-1726.

[18] Holderied A and Anders HJ. Animal models of kidney inflammation in translational medicine. Drug Discov Today Dis Models 2014; 11: 19-27.

[19] Le Clef N, Verhulst A, D'Haese PC and Vervaet BA. Unilateral renal ischemia-reperfusion as a robust model for acute to chronic kidney injury in mice. PLoS One 2016; 11: e0152153.

[20] Basile DP, Donohoe D, Roethe K and Osborn JL. Renal ischemic injury results in permanent damage to peritubular capillaries and influences long-term function. Am J Physiol Renal Physiol 2001; 281: F887-899.

[21] Landini G, Martinelli G and Piccinini F. Colour deconvolution-stain unmixing in histological imaging. Bioinformatics 2020; 37: 1485-1487.

[22] Ruifrok AC and Johnston DA. Quantification of histochemical staining by color deconvolution. Anal Quant Cytol Histol 2001; 23: 291-299.

[23] Jang HR, Park JH, Kwon GY, Lee JE, Huh W, Jin HJ, Choi SJ, Oh W, Oh HY and Kim YG. Effect of preemptive treatment with human umbilical cord blood-derived mesenchymal stem cells on the development of renal ischemia-reperfusion injury in mice. Am J Physiol Renal Physiol 2014; 307: F1149-1161.

[24] Ascon DB, Lopez-Briones S, Liu M, Ascon M, Savransky V, Colvin RB, Soloski MJ and Rabb H. Phenotypic and functional characterization

of kidney-infiltrating lymphocytes in renal ischemia reperfusion injury. J Immunol 2006; 177: 3380-3387.
[25] Ascon M, Ascon DB, Liu M, Cheadle C, Sarkar C, Racusen L, Hassoun HT and Rabb H. Renal ischemia-reperfusion leads to long term infiltration of activated and effector-memory T lymphocytes. Kidney Int 2009; 75: 526-535.
[26] Wang J. Neutrophils in tissue injury and repair. Cell Tissue Res 2018; 371: 531-539.
[27] Jang HR and Rabb H. The innate immune response in ischemic acute kidney injury. Clin Immunol 2009; 130: 41-50.
[28] Jung M, Sola A, Hughes J, Kluth DC, Vinuesa E, Viñas JL, Pérez-Ladaga A and Hotter G. Infusion of IL-10-expressing cells protects against renal ischemia through induction of lipocalin-2. Kidney Int 2012; 81: 969-982.
[29] Tögel F, Zhang P, Hu Z and Westenfelder C. VEGF is a mediator of the renoprotective effects of multipotent marrow stromal cells in acute kidney injury. J Cell Mol Med 2009; 13: 2109-2114.
[30] Fu Y, Tang C, Cai J, Chen G, Zhang D and Dong Z. Rodent models of AKI-CKD transition. Am J Physiol Renal Physiol 2018; 315: F1098-F1106.
[31] Skrypnyk NI, Harris RC and de Caestecker MP. Ischemia-reperfusion model of acute kidney injury and post injury fibrosis in mice. J Vis Exp 2013; 50495.
[32] Shiva N, Sharma N, Kulkarni YA, Mulay SR and Gaikwad AB. Renal ischemia/reperfusion injury: an insight on in vitro and in vivo models. Life Sci 2020; 256: 117860.
[33] Polichnowski AJ, Griffin KA, Licea-Vargas H, Lan R, Picken MM, Long J, Williamson GA, Rosenberger C, Mathia S, Venkatachalam MA and Bidani AK. Pathophysiology of unilateral ischemia-reperfusion injury: importance of renal counterbalance and implications for the AKI-CKD transition. Am J Physiol Renal Physiol 2020; 318: F1086-F1099.
[34] Tanaka S, Tanaka T and Nangaku M. Hypoxia as a key player in the AKI-to-CKD transition. Am J Physiol Renal Physiol 2014; 307: F1187-1195.
[35] Fuquay R, Renner B, Kulik L, McCullough JW, Amura C, Strassheim D, Pelanda R, Torres R and Thurman JM. Renal ischemia-reperfusion injury amplifies the humoral immune response. J Am Soc Nephrol 2013; 24: 1063-1072.
[36] Zager RA, Johnson AC and Lund S. Uremia impacts renal inflammatory cytokine gene expression in the setting of experimental acute kidney injury. Am J Physiol Renal Physiol 2009; 297: F961-970.
[37] Lee SA, Cozzi M, Bush EL and Rabb H. Distant organ dysfunction in acute kidney injury: a review. Am J Kidney Dis 2018; 72: 846-856.
[38] Kierulf-Lassen C, Nielsen PM, Qi H, Damgaard M, Laustsen C, Pedersen M, Krag S, Birn H, Norregaard R and Jespersen B. Unilateral nephrectomy diminishes ischemic acute kidney injury through enhanced perfusion and reduced pro-inflammatory and pro-fibrotic responses. PLoS One 2017; 12: e0190009.
[39] Nishioka S, Nakano D, Kitada K, Sofue T, Ohsaki H, Moriwaki K, Hara T, Ohmori K, Kohno M and Nishiyama A. The cyclin-dependent kinase inhibitor p21 is essential for the beneficial effects of renal ischemic preconditioning on renal ischemia/reperfusion injury in mice. Kidney Int 2014; 85: 871-879.
[40] Wei J, Zhang J, Wang L, Jiang S, Fu L, Buggs J and Liu R. New mouse model of chronic kidney disease transitioned from ischemic acute kidney injury. Am J Physiol Renal Physiol 2019; 317: F286-F295.
[41] Zhang J, Wang X, Wei J, Wang L, Jiang S, Xu L, Qu L, Yang K, Fu L, Buggs J, Cheng F and Liu R. A two-stage bilateral ischemia-reperfusion injury-induced AKI to CKD transition model in mice. Am J Physiol Renal Physiol 2020; 319: F304-F311.